SAND2022-13485J

Background measurement methods for opacity experiments conducted at the Z facility

G. S. Dunham,[1] T. Nagayama,[1] J. E. Bailey,[1] and G. P. Loisel[1]

[1] *Sandia National Laboratories, Albuquerque, NM 87123, USA*

Corresponding author: gsdunha@sandia.gov

(Presented XXXXX; received XXXXX; accepted XXXXX; published online XXXXX)

Laboratory experiments typically test opacity models by measuring spectrally-resolved transmission of a sample using bright backlight radiation. A potential problem is that any unaccounted background signal contaminating the spectrum will artificially reduce the inferred opacity. Methods developed to measure background signals in opacity experiments at the Sandia Z facility are discussed. Preliminary measurements indicate backgrounds are 9-11% of the backlight signal at wavelengths less than 10 Å. Background is thus a relatively modest correction for all Z opacity data published to date. Future work will determine how important background is at longer wavelengths.

I. Introduction

Laboratory astrophysics experiments typically test opacity models by volumetrically heating a sample with x-rays. Viewing a bright backlight with and without the sample using a spectrometer[1,2,3] measures the spectrally-resolved transmission. The opacity is inferred from the natural log of the transmission divided by the sample areal density. The true transmission is

$$T_\nu^{true} = \frac{I_\nu}{I_0} = \exp(-\kappa_\nu \rho L), \quad (1)$$

where, I_ν and I_o are the attenuated and unattenuated spectra, respectively, κ_ν is the opacity, and ρL represents the areal density. In this paper we assume the plasma is spatially uniform[4] along the path length.

Background is defined here as additional signal not part of the intended measurement. The measured transmission is

$$T_\nu^{measured} = \frac{I_\nu + B}{I_0 + B} \neq \exp(-\kappa_\nu \rho L), \quad (2)$$

where I_ν+B and I_o+B represent the attenuated and unattenuated spectra including an unknown background signal, respectively. We assume background is the same in I_ν and I_o. This assumption should be valid for our experiments, but we cannot preclude the possibility that backgrounds might be different in other cases.

Sources of potential background radiation likely exist in many opacity experiments[3,5,6,7,8,9]. Backgrounds can arise from many sources, including sample self-emission, emission from nearby unresolved plasmas, high-order crystal reflections, high energy x-rays, instrument fluorescence, and glowing plasma with duration longer than the backlight. Experimenters typically reduce backgrounds as much as possible, since impacts on opacity measurement accuracy grow as the background increases. Complete elimination of background is rarely achieved and methods to quantify it are crucial.

An uncorrected background signal artificially reduces the inferred opacity. The reduction depends on the background intensity, the backlight intensity, and the transmission value that is to be measured. Figure 1 illustrates these dependencies using synthetic absorption spectra calculated using PrismSPECT[10]. Panel A shows synthetic Mg absorption spectra backlit by a high intensity source (red), and panel B shows the absorption by the same Mg plasma, but backlit by a low intensity source (blue). In both panels, the long-dashed lines represent the unattenuated backlight intensity spectra. The orange short-dashed line represents a 15 J/sr/Å background. Red and blue curves in panel C show the transmissions determined by dividing attenuated spectra by the unattenuated spectra from panels A and B, respectively. These spectra are computed without subtracting the background of 15 J/sr/Å. Since the background contamination is not removed, the inferred transmission spectra are slightly higher than the true transmission spectrum (black). Panel D shows the opacity spectra corresponding to the transmission plots. The true opacity (black) is higher than the results without any background correction. The influence of background is

greater when background is a higher fraction of the backlight intensity.

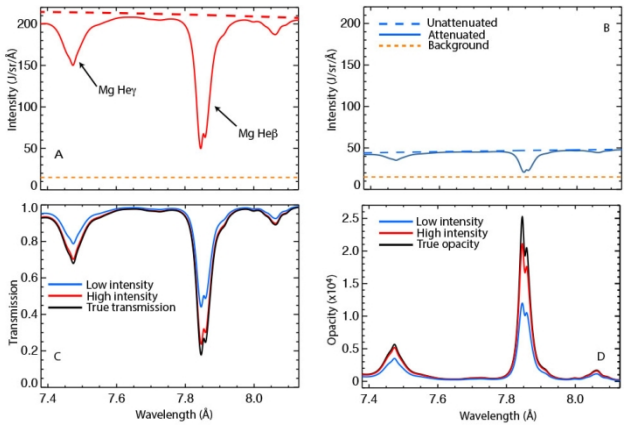

Figure 1:Background influence on transmission and opacity, illustrated using synthetic Mg plasma absorption spectra. A: synthetic attenuated and unattenuated spectra including a 15 J/sr/Å background signal. B: same absorption spectra but with significantly weaker backlight. C: impact of background on inferred transmission spectra. Red and blue are the inferred transmission from panels A and B, respectively, without accounting for background. D: the impact of background on opacity. Black curves in panels (c) and (d) are the true transmission and true opacity, respectively.

The impact of background is also worse for lower transmission (Figure 2). In Figure 2, the background signal is defined as a percentage of the unattenuated backlight signal. For a given background signal a synthetic spectrum calculation illustrates the effect on the measured opacity for different parts of the spectrum. For a deep absorption feature such as Mg He-β with a low transmission, T=0.18 (or optical depth τ=1.7), a 10% background causes a 40% change in opacity. The same 10% background signal results in a 13% reduction in opacity for the Mg Heγ since it has higher transmission, T=0.68 (or τ=0.39). All values were at line center. The continuum region in between the Mg Heγ and Mg Heβ has even higher transmission T=0.96 (or τ=0.039) and consequently the background introduces the smallest opacity error of the three. These quantitative values vary according to their transmissions, which depend in turn on areal density, line width, and the absorbing atomic populations. Nevertheless, even modest (~10%) background signal can lead to significant downward errors in the inferred opacity. This implies that, as background increases, the requirement for background determination accuracy also increases.

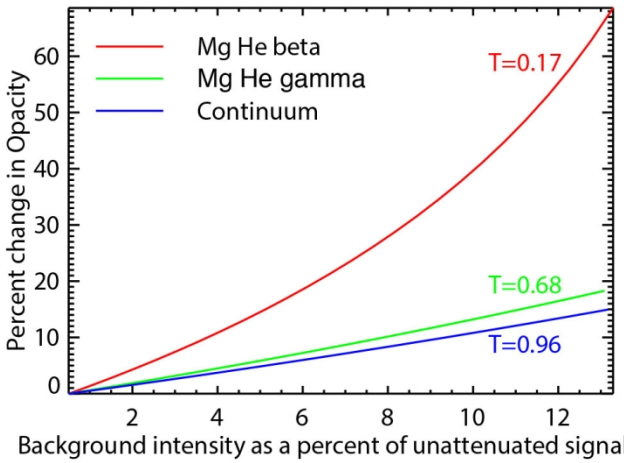

Figure 2: Opacity error as a function of background intensity, expressed as a function of the percent of unattenuated signal. The opacity error corresponds to line center for the Mg He-β and He-γ transitions, and to λ=7.59–7.76 Å for the continuum.

In reference [3] we reported severe model-data discrepancies[3]. We found that the measured opacities were significantly higher than the modeled opacities. Since we assumed that the background was negligible and did not account for it, the true opacity could be slightly higher and the discrepancy could be even worse. Knowing the background level and its impact on inferred opacity is one of the crucial steps for benchmark opacity experiments.

The remainder of this paper will present the Z experiments and evidence of background contamination in Sec. II, Analysis methods in Sec. III, Results in Sec. IV and a Discussion in section V.

II. Z experiments and evidence of background contamination

Methods to measure background depend on the experiment configuration. Figure 3 (top) schematically describes the experiment geometry at Z. The Z dynamic hohlraum radiation source[2] emits x-rays from a bright core which falls off in intensity as radius increases. The Z x-rays act to both heat and backlight the sample. From the sample point of view, Z provides the heating radiation. From the spectrometer's point of view, it works as a backlighter. Four spectrometers are fielded simultaneously at ±9° with respect to the z-pinch axis and record slit-imaged spatially-resolved x-ray spectra on Kodak RAR 2492 film. The record is time-resolved by the ~3 nsec duration of the backlighter emission. The target is split into two regions, with and without an FeMg opacity sample. Slits provide spatial resolution along the horizontal direction in Figure 3, and spectra can be extracted at any horizontal location from both angles. This configuration measures attenuated and

unattenuated spectra in every experiment, from a variety of different backlighter intensities. All information needed to infer background is recorded in a single shot, even though the most accurate transmission analysis uses an ensemble of unattenuated spectra accumulated from multiple calibration experiments, as described in Refs. 2, 14. Synthetic FeMg spectra calculated using PrismSPECT[10] are shown in the bottom panel of Figure 3. The solid curves represent the attenuated spectra seen by the ±9° spectrometers while the dashed lines represent the unattenuated spectra.

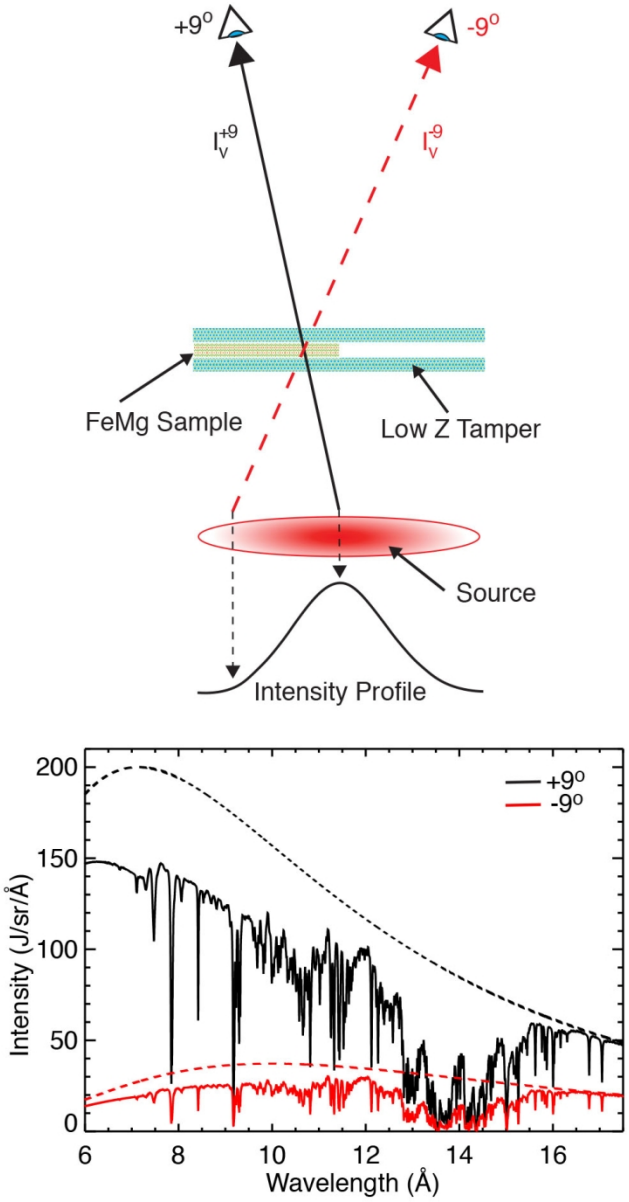

Figure 3: Top panel: Opacity measurement configuration (not to scale). Spatially-resolved spectra are recorded on four slit-imaged spectrometers at ±9°. For clarity, only one line of sight at each angle is indicated. From the spectrometer view, source intensity varies with radius. The source is approximated as a disk with ~ 400 μm radius (hwhm) with a 2000 μm outer limiting radius. The source-to-sample separation is 1000 – 2000 μm, depending on the experiment. Solid line from source to detector represents peak source intensity. Dashed line is from the lower intensity outer regions of the source. The geometry dictates that the +9° and -9° spectrometers view the peak source intensity through sample regions with and without the FeMg, respectively. Finite source to sample distances help the two spectrometers view different backlight locations. The exact location in the FeMg

sample viewed by the +9° spectrometer at peak source intensity is backlit by a lower intensity portion of the source as viewed by the -9° spectrometer (point where lines cross). Bottom panel shows synthetic FeMg spectra. Solid lines are the attenuated spectra recorded by the ±9° spectrometers shown in the top panel. The dashed lines represent the unattenuated spectra passing through the low z tamper material only.

Transmission spectra measured by the ±9° spectrometers indicate that there are notable background signals to be corrected. We extracted the spectra at the same location of the FeMg sample as indicated by Figure 3. The emergent spectra contain the same FeMg transmission, but backlit with two different intensities. Figure 4 (a) shows an example of such spectra over Mg He-α and its satellite lines from our experiments. The +9° data shows higher intensity than -9° data, as expected. Figure 4 (b) shows a comparison of the line transmission for the same case. Line transmission refers to the transmission spectrum corresponding only to the bound-bound feature, as defined in Ref. [2, 12, 14] and in the text below. The one with brighter backlighter (+9°) shows deeper Mg He-α line transmission than that with low intensity backlighter (-9°). As suggested by Figure 1 (c), this is a strong indication that background is contaminating our absorption spectra.

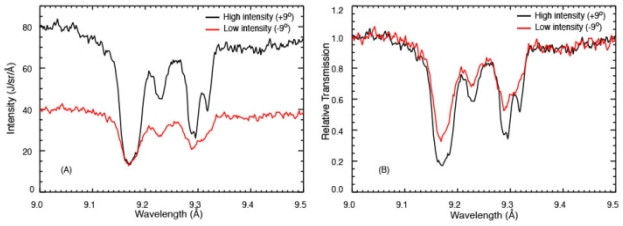

Figure 4: Mg He-α absorption (A) and line transmission (B) spectra comparing high and low intensity data from actual experimental data. The discrepancy in transmission seen at the line centers is evidence that this particular experiment shows evidence of background contamination.

The transmission measured at ±9° can be written as:

$$T_m^{+9} = \frac{I_{Am}^{+9^\circ}}{I_{Um}^{+9}} \qquad T_m^{-9} = \frac{I_{Am}^{-9}}{I_{Um}^{-9}}, \tag{3}$$

where the subscripts A and U refer to the signal attenuated and unattenuated by the opacity sample, respectively.

The signals recorded at each spectrometer are:

$$I_{Am}^{+9^\circ} = T_t {I_0}^{+9^\circ} + B \qquad I_{Am}^{-9^\circ} = T_t I_0^{-9^\circ} + B$$

$$I_{Um}^{+9\,\circ} = {I_0}^{+9^\circ} + B \qquad I_{Um}^{-9\,\circ} = I_0^{-9^\circ} + B \tag{4}$$

where T_t is the true transmission, I_o is the backlight signal, B is the background, and the subscript m denotes measured quantities. The unattenuated signal passing through the sample is comprised of the backlight ($I_0^{\pm 9^\circ}$) plus an unknown background signal (B). The unattenuated signals $I_{Um}^{+9\,\circ}$ and $I_{Um}^{-9\,\circ}$ can be deduced from the data, as described below. Furthermore, we measure the attenuated signals $I_{Am}^{+9^\circ}$ and $I_{Am}^{-9^\circ}$. A priori, we do not know the true transmission T_t, the unattenuated signals without background contamination ${I_0}^{+9^\circ}$ or $I_0^{-9^\circ}$, or the background B. However, the four measured quantities $I_{Am}^{+9^\circ}$, $I_{Am}^{-9^\circ}$, I_{Um}^{+9}, and I_{Um}^{-9} enable us to determine the background B in multiple ways. The remainder of this paper describes the methods to quantify the background.

III. Analysis methods

We developed two methods to determine the background. The first method is called the Dual Backlight Intensity (DBI) method. This method takes advantage of the fact that the transmissions inferred from two spectra backlit with different intensities agree with each other only when the correct amount of background is removed. The second method is called the Model-Data Comparison (MDC) method. This takes advantage of the fact that measured and modeled spectra agree at line centers only when the correct amount of background is removed from the measured spectra. The second approach assumes that modeled spectra are correct, therefore, is applicable to relatively well-understood Mg spectra in our case. These two approaches provide independent assessment of the background from our experimental data.

Both the DBI and MDC methods require knowledge of the unattenuated spectrum I_{Um}^{+9} and $I_{Um}^{-9\,\circ}$. The unattenuated spectrum I_{Um}^{+9} is deduced by a variety of means in order to infer the absolute transmission[2,3,13]. However, the background measurement described here uses "relative transmission" defined in the similar manner to "line transmission" described in Ref. [2, 12, 14]. Using relative transmission *to determine background* provides notable simplification and accuracy. We describe the relative transmission determination and DBI method first and return to the MDC method in the following section.

III-(a). Relative transmission and Dual Backlight Intensity (DBI) method

The meaning of relative transmission is clarified by example. Figure 5A shows synthetic attenuated spectra for the Mg He-β from two different backlight brightnesses with 20 J/sr/Å added to simulate unaccounted background contamination. Two reference wavelength points are selected at relatively high transmission, so that the region in-between these points is at lower intensity (Figure 5A). These points are used to define a line, which becomes a *reference spectrum* to define the relative transmission.

The relative transmission T_r is then defined as $T_r = I_A/I_R$, where I_A and I_R are the attenuated and the reference spectrum, respectively. We assert that the relative transmission defined by a straight reference spectrum is as accurate as absolute transmission to constrain the background level. We test this hypothesis by demonstrating the idea of the DBI method below. However, we also must emphasize that this refers only to background determination and the ultimate goal of absolute opacity measurements still requires absolute transmission [see 1,2,13].

As a specific example, consider the synthetic Mg spectrum in Figure 5A. The straight-line approximation to the relative transmission is defined by the points at the wavelengths of 7.64Å and 8.16Å and the intensity values of the absorption spectrum at these wavelengths and are marked in panel (A) by red and black dots.

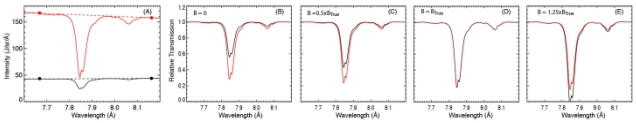

Figure 5: (A) Synthetic Mg absorption spectra from high and low intensity backlight with 20 J/sr/Å of background contamination added. The dashed red and black lines correspond to the reference spectra (see text). Panel B shows the data converted to relative transmission where disagreement is seen in at line center due to the additional background. (C) Improved but still poor agreement when 10 J/sr/Å of background is accounted for. (D) Perfect agreement with the correct 20 J/sr/Å background signal accounted for. (E) Overcorrection when 25 J/sr/Å is accounted for.

The solid curves are divided by the dashed lines in Figure 5(A) to determine the relative transmission for these spectra shown in Figure 5(B). The relative transmission spectra disagree when background remains unaccounted for.

Figure 5 panels C, D, and E show how relative transmission agreement varies as subtracted background level increases. When too little background is subtracted the agreement remains inadequate (Figure 5(C)). When the correct background level is subtracted, the relative transmissions agree (Figure 5(D)). If too much background is removed, the relative transmission agreement deteriorates (Figure 5(E)).

Why is relative transmission so useful to determine background contamination? The reason is that sensitivity to the background depends on transmission values as shown in Figure 2. This relative transmission technique forces high-transmission points (i.e., x=7.64Å and 8.16Å) to agree, simultaneously enabling a determination of whether the spectra at lower transmission also agree. If the background is successfully removed, the lower transmission regions between the end points of the straight line also agree (Figure 5D). If not, they show disagreement as in Figure 5B, C, and E.

The relative-transmission concept was illustrated above using relatively simple Mg K-shell spectra, but is equally applicable to complex spectra with many blended lines such as Fe L-shell spectra. The synthetic Fe L-shell data in Figure 6 depict the identical steps shown previously for Mg K-shell data. The only difference in implementation is a different choice of end points to define the reference spectra. Line end points were chosen at 12.73Å and 13.24Å which define the local high intensity points bounding a feature of interest. The relative transmissions from the high intensity and low intensity backlighters agree only when the correct background subtraction is performed (Figure 6(d)).

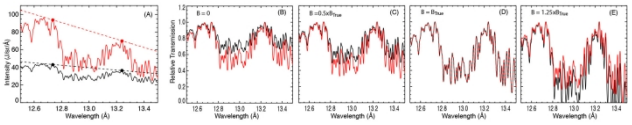

Figure 6: Synthetic Fe L-shell spectra illustrating that relative transmission is also applicable to complex spectra with many blended lines. Background quantities and the progression of correction values are identical to Figure 5. Line end points defining the reference spectrum were selected at 12.73Å and 13.24Å in this case, marked in panel (a) as red and black dots.

Examining transmission calculated from synthetic Mg absorption spectra with two different brightnesses of backlight shows how background-corrected transmission changes as a function of subtracted background (Figure 7A). This example assumed sample transmission of 0.2, backlit by two different brightnesses of 100 and 20 J/sr/Å and then 20 J/sr/Å background is added. The background-corrected measured transmission is

$$T_{cm} = \frac{(I_o \, x \, T_T + B_T) - B_i}{(I_o + B_T) - B_i}, \quad (3)$$

where the quantity I_o is the unattenuated backlight signal, T_T is the true transmission and the quantity (I_o x T_T) + B_T represents the measured attenuated signal, where B_T is the true background. The variable B_i is the trial background intensity subtracted from the synthetic data. Figure 7A shows inferred transmissions as a function of subtracted background. When no background is subtracted, the inferred transmissions are very different for the two backlight intensity cases shown at B_i=0 in Figure 7A. Subtracting background improves the agreement in the inferred transmission, until the trial background value becomes larger than the true background. When the correct background intensity value (20 J/sr/Å) is subtracted, the two

inferred transmissions agree at the true transmission (i.e., 0.2 here).

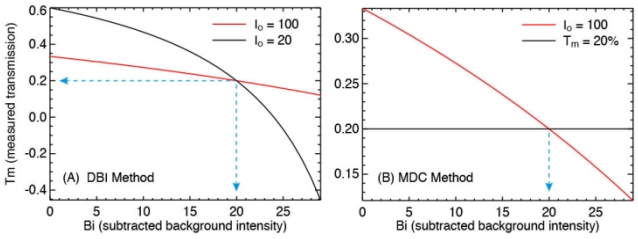

Figure 7: Measured transmission varies with background intensity. (A) The difference between the measured and true transmission is more pronounced for lower intensity backlight signals because background intensity is a larger proportion of the attenuated signal. (B) Model transmission of 0.2. Discrepancy between model and data decreases as the true background is approached.

We use this principle, as described previously in this section, to search for a background intensity. For example, we have absorption spectra measured with two backlight brightnesses (e.g., Figure 3 & Figure 4 (A)). We search for the B_i value that renders the relative transmission (Eq. (3)) measured with the two backlight intensities equal.

The following process is executed to implement the DBI method. First, determine a reasonable array of background intensity values to subtract from I_v and I_o. Then, infer the relative transmission as described above for each background intensity value. An upper bound on potential background intensity values is given by the minimum intensity of the deepest spectral feature. Subtracting a value larger would result in an unphysical negative transmission. The difference between the spectral features recorded with high and low intensity backlight, measured in relative transmission units at their local minimum near line center, is tabulated against the subtracted background intensity value. The value yielding the smallest difference between the low and high intensity spectra is taken as the optimum background intensity value. A result from the DBI method for the Mg He-α using the ±9° spectrometer views is shown in Figure 8. Panel A shows the uncorrected relative transmission indicating a background correction is required. Panel B shows the corrected spectra with 13.8 J/sr/Å of background intensity removed from both spectra prior to converting to relative transmission. Note the optimum background correction value was determined at the deep line center of the Mg He-α. The result is not optimized for the satellite lines at slightly higher wavelength. The process is repeated for all available spectral features, yielding a set of background intensity correction values at discrete wavelengths. For this work, measurements were averaged and the standard deviation taken as the uncertainty.

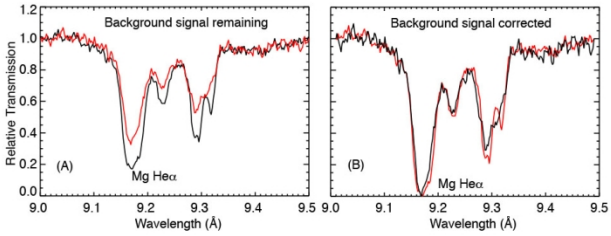

Figure 8: Results of DBI method for the Mg He-α absorption spectra showing a comparison of experimental spectrum from both high and low intensity backlight spectra. (A) Uncorrected relative transmission. (B) Background corrected relative transmission. Black line is the high intensity spectra from the +9o spectrometer. Red line is the low intensity spectra from the -9o spectrometer.

The DBI method assumes that the background is the same at +/- 9. The validity of this assumption depends on what causes the background. If the background comes from the sample self-emission, it should be the same in both data since the spectra are taken at exactly the same location in the sample, marked by where $I_v^{\pm 9}$ cross in Figure 3 (top). If the background originates from other sources, the background level could be slightly different at each spectrometer.

III-(b). Model-Data Comparison (MDC) method

A complementary approach compares a single experimental spectrum directly to a modeled spectrum. We refer to this as the MDC method. It has the advantage that it does not require simultaneous measurements at two backlight intensities. The disadvantage is that it assumes the modeled spectrum is accurate and the plasma conditions are accurately known. Consequently, this technique is only applicable to spectral lines from relatively simple bound-bound transitions. For example, in this paper, we apply this MDC method to Mg K-shell transitions.

In the MDC method, we assume that the relative transmission given by the model is accurate and we search for the background that renders the inferred experimental transmission to agree with the modeled transmission (Figure 7B). The modeled relative transmission does not contain background and remains constant. Similar to the DBI method, an array of background subtraction values is subtracted from the attenuated and the reference spectra, searching the background that minimizes the difference between the model and data. When the correct background is subtracted, the inferred relative transmission agrees with the modeled relative transmission. We reiterate that these inferred/modeled transmissions are *relative* values used for the background determination only and are not substitutes for the absolute sample opacity transmission results.

Figure 9 shows a sample experimental intensity spectrum with its corresponding model prediction converted to relative transmission. The red curve represents the experimental data and the black curve is the model. The left panel shows the uncorrected spectrum where the discrepancy at the deep line centers for the Mg He-β and He-γ are notable. The right panel shows the same spectrum after accounting for the background intensity minimizing the difference between model and data. The agreement in deep line centers is improved while the continuum regions show little effect from this correction.

As described earlier, the MDC method has a significant limitation, i.e., it assumes that the modeled spectrum is accurate. Accuracy of oscillator strengths, blended satellite line intensities, and line widths in the model can affect the results. Furthermore, any inaccuracies in plasma conditions (temperature, density, and areal density), line shapes, and instrument broadening between model and data can also contribute to observed transmission differences, in addition to background. However, these problems can be mitigated by using multiple strong bound-bound line features. Using multiple lines improves accuracy since model deficiencies are likely different for different lines. Also, the strongest Mg lines in the experiments shown here have optical depths greater than ~3 and the transmission at line center is essentially zero before the line is convolved with the instrument response. Thus, the background analysis using such strong lines are less sensitive to the inaccuracies listed above. Multiple factors influence the uncertainty of background determination and a thorough evaluation of those different contributions is beyond the scope of this paper. Nevertheless, a future study examining the dependence of background on different spectral models would be valuable. Due to the fact there are a number of factors that influence the uncertainty of each and every line we rely on the mean and standard deviation determined from as many lines as possible.

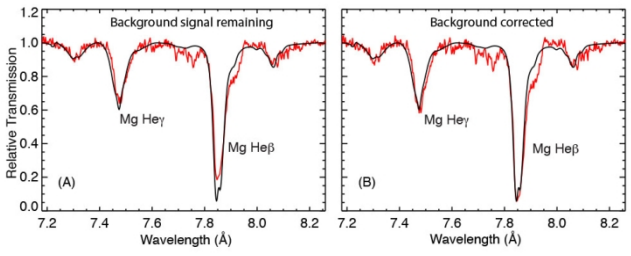

Figure 9: Comparison of experimental spectrum to model prediction for the Mg He-γ and He-β. Experimental data prior to background correction(A). Same data corrected for background (B). The red curve is the experimentally determined relative transmission, the black curve is the model.

IV. RESULTS

Analysis was performed for a set of 5 experiments at approximately T_e = 182 eV and n_e=3x10^{22} e$^-$/cm^3(defined in Ref. 2 as "Anchor 2" conditions). Up to 4 spectral features were analyzed per experiment yielding background intensity correction values at the wavelength of each line center.

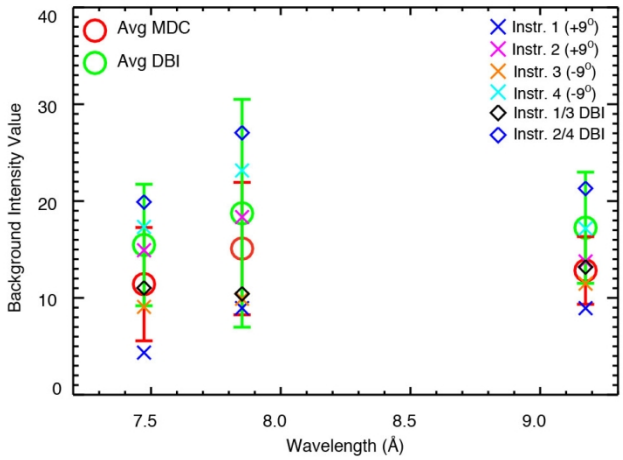

Figure 10: Background correction values in intensity units for both the DBI and MDC methods for shot z2874. Included are MDC results from 4 instruments marked as X's. Diamonds denote the DBI results which are from comparing instruments 1 and 3 and instruments 2 and 4. Measurements at a single wavelength were averaged with error bars representing their standard deviation.

Figure 10 presents the results for one experiment, shot z2874. The open circles represent the average values for each method. As described above, two spectrometers at +9° and two spectrometers at -9° each simultaneously observes the source, recording spatially-resolved spectra from a continuous range of source intensities. Low and high intensity spectra are extracted from the data, yielding a total of 4 simultaneous measurements to compare against model data. The DBI method requires two measurements with different intensities, resulting in only two measurements for each shot. The differences between measurements at different wavelengths are comparable to the standard deviation. The two methods agree to within the standard deviation when averaged over wavelength, with mean values of 13±2 and 17±2 J/sr/Å for the MDC and DBI methods, respectively.

The lines included here are Mg He-alpha (1s2-1s2p), beta (1s2-1s3p), gamma (1s2-1s4p). The background in each experiment is then determined by computing the mean and standard deviation of background values determined from all the listed lines. For the conditions in these

experiments, He-like lines are advantageous for background measurements since He-like ions dominate, and the population depends weakly on any condition inaccuracy or condition changes with time. In contrast, H-like populations are sensitive to small condition changes. Furthermore, difficulties in H-like Ly-alpha line profile modeling introduces additional uncertainties for the MDC method. Nevertheless, we performed background measurements with the H-like lines in order to help evaluate their reliability. These measurements showed that including the H-like lines changes the mean background value by less than the standard deviation. While reassuring, we elected not to include the H-like line results here, pending a more complete understanding of the problems described above.

Both methods were applied to four additional experimental data sets. Background intensity correction values found at each wavelength are shown in Figure 11. The open symbols represent the average background intensity correction value from all shots at a given wavelength. The triangles are results from the DBI method while the circles are from the MDC method. Data from each shot is color coded according to the legend. Background correction values averaged over all measurements for each shot are presented in Table 1 as intensity values and as a percentage of the unattenuated signal (I_o). The maximum background determined from the minimum intensity of the deepest spectral feature is also provided. The average values for the DBI and MDC methods agree within the errors. The background correction was found to be 8% or 10% of the unattenuated signal level for the MDC and DBI methods, respectively. The value of I_o used to determine the percentage was the absolute unattenuated intensity, averaged over the wavelength region defined for each line.

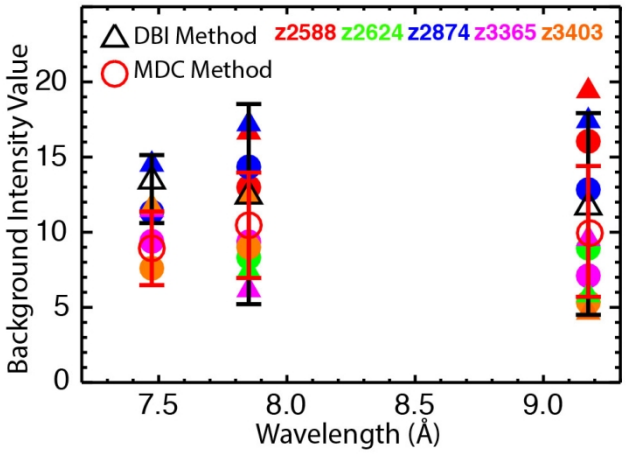

Figure 11:Results for background subtraction values found for 5 experiments. DBI method results – triangles. MDC method results – circles. Open symbols represent average of measurements for each method with 1standard deviation errors. Background intensity in units of J/sr/Å.

Table 1: Background intensity values found for 5 experiments at Anchor 2 conditions. Values are presented in both intensity units of J/sr/Å and in percent of the unattenuated signal, I_o. The value for each shot represents the average across all wavelengths for each method. The maximum background value based on the intensity of the deepest absorption feature is provided in the last column.

	DBI		MDC		Max bkg from data
Z shot No.	Bkg. value	% of I_o	Bkg. value	% of I_o	
Z2588	19±1	17±2	15±2	13 ±2	18
Z2624	6±0.2	5±0.2	8±1	7±2	9
Z2874	17±2	10±2	13±2	7±1	16
Z3365	8±5	9±4	8±1	8±3	8
Z3403	10±4	14±4	7±1	8±3	5
Average	12±2	11±2	10±1	9±2	

V. DISCUSSION

The agreement between both approaches, and between the individual measurement values, bolsters confidence in these methods for determining the background contamination level. The background is approximately the same on 4 out of 5 experiments, suggesting that the background origin is similar on these experiments. The background variation between different wavelengths is comparable to the measurement standard deviation (Fig. 10), suggesting that using a constant background approximation over this wavelength range is adequate. Further work is needed to evaluate background variation at longer and shorter wavelengths. Finally, we note that an initial background estimate can be obtained by using the maximum possible background consistent with knowledge that the background can be no larger than the minimum intensity at the center of the strongest lines. The implementation of the two methods described here provides evidence that this is a reasonable approximation, rather than strictly an upper bound.

We found that typical background level in Z opacity experiments is about 9-11% of the backlight signal with measurement uncertainty of roughly 30%. This means we can determine the background signal accurately within 2-3% of the backlight signal.

This background is already accounted for in the results published in Ref [2]. Evidence for background was cited in Ref. [3], but it was not accounted for. The exact opacity correction depends on the transmission (Figure 2). We are currently working on refining the iron results using the improved analysis methods including the background determination methods described here.

Only Mg K-shell spectral lines were examined for the results presented here. The same approach will be systematically applied to Fe K-shell spectra at wavelengths greater than 9.5 Å, and to Ni, Cr, and O data as well. Furthermore, background will be determined for data acquired at both higher and lower temperatures, densities, and areal densities. Trends in background intensity as a function of wavelength, element, and plasma conditions may help identify the origin of the existing background contamination and thus enable future reductions in the background. In principle, the methods developed here are not limited to Z opacity measurements. They are applicable to any absorption spectra where an unknown background contamination signal may be present.

VI. ACKNOWLEDGEMENT

The authors would like to thank Daniel Mayes for his help in reviewing the manuscript. The authors would also like to thank the Z operations team, and in particular the diagnostic fielding team for their continued excellent support and attention to detail required to acquire the opacity data discussed in this work. Finally, we would like to thank the Z facility management team for their continued support of the opacity experiment platform.

This paper describes objective technical results and analysis. Any subjective views or opinions that might be expressed in the paper do not necessarily represent the views of the U.S. Department of Energy or the United States Government.

Sandia National Laboratories is a multi-mission laboratory managed and operated by National Technology and Engineering Solutions of Sandia, LLC., a wholly owned subsidiary of Honeywell International, Inc., for the U.S. Department of Energy's National Nuclear Security Administration under contract DE-NA0003525.

VII. DATA AVAILABILITY STATEMENT

The data that support the findings of this study are available from the corresponding author upon reasonable request.

VIII. REFERENCES

[1] J. E. Bailey, G. A. Rochau, R. C. Mancini, C. A. Iglesias, J. J. MacFarlane, I. E. Golovkin, C. Blancard, Ph. Cosse, and G. Faussurier, *Phys. Plasmas* **16,** 058181 (2009)

[2] T. Nagayama et al., *Physical Review Letters* **122**, 235001 (2019)

[3] J. E. Bailey et al., *Nature* (London) 517, **56** (2015)

[4] T. Nagayama, J. E. Bailey, G. Loisel, S. B. Hansen, G. A. Rochau, R. C. Mancini, J. J. MacFarlane, I. Golovkin, Phys. Plasmas **21**, 056502 (2014)

[5] T. S. Perry et al., *Physical Review E* **54**, 5617 (1996)

[6] R. F. Heeter et al., *J. Plasma Phys.* (2017), vol. **83**, 595830103 (2017)

[7] P. T. Springer et al., *J. Quant. Spectrosc. Radiat. Transfers 51 371 (1994)*

[8] C. A. Iglesias, J. Quant. Spectrosc. Radiat Transfers 99 295 (2006)

[9] J. -C Pain, F. Gilleron, High Energy Density Physics 34 100745 (2020)

[10] *Prism Computational Sciences, Inc., PrismSPECT Version 7.0.0 computer program, https://www.prism-cs.com.*

[11] T. Nagayama, Bailey, J. E., Loisel, G. P., Rochau, G. A, MacFarlane, J. J., Golovkin, I. E., *Physical Review E* **95**, 063206 (2017)

[12] T. Nagayama, Bailey, J. E., Loisel, G. P., Hansen S. B., Rochau, G. A, Mancini, R. C., MacFarlane, J. J., Golovkin, I. E., *Phys. Plasmas* **21**, 056502 (2014)

[13] J. E. Bailey et al., *Physical Review Letters* **99**, 265002 (2007)

[14] J. E. Bailey, G. A. Rochau, R. C. Mancini, C. A. Iglesias, J. J. MacFarlane, I. E. Golovkin, J. C. Pain, F. Gilleron,C. Blancard, Ph. Cosse, G. Faussurier, G. A. Chandler, T. J. Nash, D. S. Nielsen, and P. W. Lake, *Review of Scientific Instruments* **79**, 113104 (2008).